ORIGINAL ARTICLE

TIMP1 preserves the blood−brain barrier through interacting with CD63/integrin *β*1 complex and regulating downstream FAK/RhoA signaling

Jingshu Tang, Yuying Kang, Longjian Huang, Lei Wu, Ying Peng[*]

State Key Laboratory of Bioactive Substances and Functions of Natural Medicines, Institute of Materia Medica, Chinese Academy of Medical Sciences & Peking Union Medical College, Beijing 100050, China

Abstract   Blood−brain barrier (BBB) breakdown and the associated microvascular hyperpermeability are hallmark features of several neurological disorders, including traumatic brain injury (TBI). However, there is no viable therapeutic strategy to rescue BBB function. Tissue inhibitor of metalloproteinase-1 (TIMP1) has been considered to be beneficial for vascular integrity, but the molecular mechanisms underlying the functions of TIMP1 remain elusive. Here, we report that TIMP1 executes a protective role on neuroprotective function *via* ameliorating BBB disruption in mice with experimental TBI. In human brain microvessel endothelial cells (HBMECs) exposed to hypoxia and inflammation injury, the recombinant TIMP1 (rTIMP1) treatment maintained integrity of junctional proteins and trans-endothelial tightness. Mechanistically, TIMP1 interacts with CD63/integrin *β*1 complex and activates downstream FAK signaling, leading to attenuation of RhoA activation and F-actin depolymerization for endothelial cells structure stabilization. Notably, these effects depend on CD63/integrin *β*1 complex, instead of the MMP-inhibitory function. Together, our results identified a novel MMP-independent function of TIMP1 in regulating endothelial barrier integrity. Therapeutic

interventions targeting TIMP1 and its downstream signaling may be beneficial to protect BBB function following brain injury and neurological disorders.

1. Introduction

The blood−brain barrier (BBB) is a unique microvascular structure that forms the major interface between central nervous system (CNS) interstitial fluids and the circulating blood. BBB disruption induces blood-derived neurotoxic proteins accumulation in the CNS, resulting in initiating and/or contributing to various neurological diseases, such as traumatic brain injury (TBI)[1,2], ischemia[3], Parkinson's disease[4], Huntington's disease[5], Alzheimer's disease[6], and multiple sclerosis[7]. BBB breakdown trigged by direct tissue loss is a hallmark of TBI, leading to edema and increased intracranial pressure followed by decreased cerebral perfusion pressure, which are important contributors to TBI pathology and poor clinical outcomes[8]. Therefore, restoring the BBB integrity is a potential therapy for CNS diseases, especially TBI[9].

The BBB is composed mainly of capillary endothelial cells (ECs) that are fused by tight junctions (TJs) and adherent junctions (AJs). The junctional proteins interact with the cytoskeletons to maintain the cell morphology and cell−cell connection, thereby stabilizing the EC structure and persevering the BBB integrity[10]. Matrix metalloproteinase-9 (MMP9) was thought to be primarily responsible for BBB breakdown due to its proteolysis activity that mediates EC junction and extracellular matrix (ECM) degradation[11]. The enzymatic activity of MMP9 is regulated by tissue inhibitors of metalloproteinase-1 (TIMP1), a secreted protein that is an endogenous inhibitor of MMP9[12]. Alteration of the TIMP1/MMP9 ratio is associated with pathological processes in various diseases[13−15]. Previous studies have shown that TIMP1 deficiency exacerbated BBB disruption in a focal cerebral ischemia model[16], whereas adenovirus-mediated gene transfer of TIMP1 rescued BBB damage with enhanced angiogenesis[17]. Moreover, mice deficient in TIMP1 exhibited increased cardiovascular permeability, and TIMP1 loss was associated with disruption of the skeletal muscle microvascular network[18]. Although there is much experimental evidence suggesting that TIMP1 has a protective effect on vascular integrity, it is not clear whether TIMP1 can attenuate BBB disruption in TBI, and the signaling mechanisms underlying TIMP1 regulation on endothelia cells remain elusive.

Previous reports proposed TIMP1 upregulation as a response to robust MMP9 increases to inhibit proteolytic degradation[12]. However, an MMP inhibitor (PD166793) did not reverse myocardial fibrosis reduction in TIMP1-deficient mice[19] and increased vascular permeability was not accompanied by greater MMP activity in $Timp1^{-/-}$ mice[18], suggesting that there may be other mechanisms involved in TIMP1-regulated vascular integrity. TIMP1 has a two-domain structure with an N-terminal region that is well-known for inhibiting MMP activity[20], and the C-terminal region exhibits cytokine activities *via* interacting with CD63, a member of tetraspanins[21]. Accumulating studies have revealed that TIMP1 binds to CD63 and forms a ternary TIMP1/CD63/integrin β1 complex, leading to the activation of integrin β1 and the downstream signaling. TIMP1 activates the PI3K pathway to induce angiogenesis and promote cell survival in several carcinomas[22,23]. The TIMP1/CD63 interaction is a driving force in promoting myocardial fibrosis *via* the nuclear translocation of β-catenin and the increased expression of ECM collagens[19]. The TIMP1/CD63 axis also plays an important role in physiological conditions, regulating the focal adhesion and cytoskeletal reorganization through FAK/PI3K signaling to trigger the spreading and migration of human neural stem cells (hNSCs)[24]. Importantly, studies have demonstrated that the two mechanisms, MMP-dependent and -independent pathways co-exist in several pathophysiological conditions, displaying a synergistic role in regulating multiple sclerosis[25,26], ovarian anomalies[27], and wound healing[28]. Based on these emerging findings, we attempt to explore whether the MMP-independent mechanism of TIMP1 is involved in regulating endothelial barrier integrity and maintaining BBB function.

Here, we report a novel mechanism of TIMP1 in regulating endothelial barrier integrity. Recombinant TIMP1 (rTIMP1) exhibited protective effects on motor function *via* ameliorating the BBB disruption in mice with experimental TBI. Using an *in vitro* BBB model composed of human brain microvessel endothelial cells (HBMECs), TIMP1 was shown to maintain junctional protein integrity and trans-endothelial tightness through binding to the CD63/integrin β1 complex and activating downstream FAK signaling, in addition to its regulation of ECM turnover and remodeling. TIMP1-induced FAK phosphorylation inhibited RhoA activity, contributing to F-actin depolymerization and EC structure stabilization. Collectively, our studies strengthen the role of TIMP1 as an effective regulator of BBB. We propose that the novel MMP-independent mechanism of TIMP1 in regulating EC integrity can contribute to rescue BBB function in neurological disease, including, but not limited to TBI.

2. Materials and methods

2.1. Animals

All animal care and experimental procedures complied with the Animal Management Rule of the Ministry of Health, People's Republic of China (document No. 55, 2001) and were approved by the Laboratory Animal Ethics Committee of Chinese Academy of Medical Science, Beijing, China. Male C57BL/6N mice were obtained at 8 weeks of age from Vital River Laboratories

Technology Co., Ltd. (Beijing, China). Animals were housed three per cage, in a temperature (21−25 °C) and humidity (45%−50%) controlled room with a 12-h light/dark cycle, and fed a standard rodent diet with water *ad libitum*.

2.2. Surgical procedures

All animals were anesthetized with isoflurane, intubated and placed in a stereotaxic frame. A craniectomy with 3-mm diameter was performed in the right hemisphere (0.8 mm posterior from bregma and 1.3 mm lateral to the sagittal suture) with a handheld trephine to expose the intact dura. A modified Feeney's weight drop injury (WDI) model was used to induce traumatic brain injury by advancing the impacting rod into the exposed right parietal cortex to a depth of 2 mm tissue, and then with 20 g falling weight from 25 cm height. After the impact, anesthesia was discontinued and the incision was promptly sutured. The sham injury mice were not subjected to the impact, but otherwise underwent similar surgical procedures. After surgery, animals were housed under the conditions mentioned above.

2.3. Rotarod test

The balance and motor activity of animal model was assessed with the accelerating rotarod (XR1514, Xinruan, Shanghai, China). The speed of rotation was gradually accelerated from 4 to 40 rpm within 3 min. Each mouse was placed on a 3.5 cm rotating rod, and the fall latency was recorded for all trials.

2.4. Beam balance test

Mice were placed individually on an elevated narrow wooden beam (6 mm wide, 1 m long, 30 cm height from floor). The latency for mice to traverse the beam and hindlimb performance (based on a 1−7 rating scale) were recorded as previously described[29,30]. The numbers of contralateral rear footfaults were also recorded[31].

2.5. Evans blue extravasation

Blood−brain barrier disruption was evaluated using Evans blue dye extravasation. At 72 h post-TBI, Evans blue dye (4% in PBS, E2129, Sigma−Aldrich, St. Louis, MO, USA) was injected *via* the tail vein at 3 mL/kg and allowed to circulate for 2 h. The mice anesthetized with isoflurane were intracardial perfused with sterile saline. Brain samples were then weighed and Evans blue dye was extracted in 1 mL formamide for 48 h at 45 °C. The concentration of Evans blue dye was measured by spectrophotometry at 620 nm.

2.6. Cell culture and reagents

HBMECs from Cell Systems (ACBRI376, Kirkland, WA, USA) were cultured in complete endothelial cell medium (1001, Sciencell, San Diego, CA, USA) in a humidified atmosphere of 5% CO_2 at 37 °C. Only up to eight passages were used for experiments. HBMECs grown to confluence were exposed to IL-1β plus hypoxia which was induced by placing the cells in the hypoxia incubator chamber (27310, Stem Cell, Vancouver, BC, Canada) and perfusing the chamber with 95% N_2 and 5% CO_2 at a rate of 20 L/min for 10 min. The chamber was sealed and kept at 37 °C for 24 h.

2.7. In vitro trans-endothelial permeability assay and trans-endothelial electrical resistance (TEER) assay

Endothelial permeability measurement was performed as previously described[32]. A total of 2.5×10^5 HBMECs were seeded onto the upper surface of the transwell chamber (12 mm diameter) with 0.4 μm pores (3460, Corning, Tewksbury, MA, USA). The transwell PET membranes were coated with 70 μg/mL collagen (354236, Corning). After reaching confluence, HBMECs were exposed to hypoxia plus 20 ng/mL IL-1β for 24 h. To assess paracellular permeability, 40-kDa FITC-dextran (FD40S, Sigma) were added into the luminal chamber at a concentration of 1 mg/mL. Fluorescence intensity was measured at excitation wavelength of 490 nm and emission wavelength of 520 nm with a fluorescence reader after 2 h by removing 40 μL media from the abluminal chamber. For TEER assay, resistance was measured by Millicell ERS-2 Epithelial Volt-Ohm Meter (Millipore, Frederick, MD, USA), according to Eq. (1):

$$TEER = (\text{resistance value of cell layers} - \text{resistance of blank filters}) \times \text{area of insert} \tag{1}$$

2.8. Transfection with cDNA or short interfering RNA

Transfections of cDNA constructs were carried out using Lipofectamine 3000 (Invitrogen, Waltham, MA, USA) following the manufacturer's instructions. The siRNAs against *TIMP1* (siRNA1, 5′-GAUCAAGAUGACCAAGAUGUA-3′ and siRNA2, 5′-CCUUAU ACCAGCGUUAUGAGA-3′), the siRNAs against integrin β1 (siβ1, 5′-CCGUAGCAAAGGAACAGCA-3′), the siRNAs against *CD63* (siCD63, 5′-ACGAGAAGGCGAUCCAUAA-3′) and the non-silencing control RNA (NC, 5′-UUCUCCGAACGUGUCACGU-3′) were purchased from GenePharma Corporation (Shanghai, China). The siRNAs and NC were transfected into cell lines using Lipofectamine 3000. Cells were incubated at 37 °C for 6 h before replaced by complete medium and cultured for an additional 48−60 h before further assays. The knockdown efficiency was verified by Western blots.

2.9. Expression and purification of recombinant TIMP1 proteins

pcDNA3.1B-TIMP1-myc-His plasmid or pcDNA3.1B-Ala-TIMP1-myc-His plasmid was constructed and transfected with lipo3000 into the HEK293T cells (American Type Culture Collection, Manassas, VA, USA) according to the manufacturer's recommended protocol. Transfected cells were cultured according to ATCC recommendations. 293T culture medium was replaced at 12 h post-transfection with DMEM (Thermo Fisher Scientific, Carlsbad, CA, USA). Culture medium that contained secreted TIMP1 or Ala-TIMP1 was collected on the sixth day after medium replacement. Recombinant TIMP1 and Ala-TIMP1 was purified using Ni Sepharose High-Performance (17-0575-01, GE Healthcare, St. Louis, MO, USA) following manufacturer's instruction. Finally, the TIMP1 protein was eluted by 500 mmol/L imidazole, and dialyzed against PBS (pH 7.2) *via* centrifugal filtration with a 3000-MW cutoff filter (MilliporeSigma, St. Louis, MO, USA). The purified recombinant TIMP1 and Ala-TIMP1 was stored at −80 °C.

2.10. Western blot analysis

Whole-cell lysates were prepared using RIPA lysis buffer (50 mM Tris−HCl, pH 7.5, 150 mmol/L NaCl, 1% Triton X-100, 1% sodium deoxycholate, 0.1% SDS, 10 mmol/L EDTA), supplemented with complete EDTA-free protease inhibitor mixtures (4693116001, Roche, Indianapolis, IN, USA) and phosphatase inhibitors (04906845001, Roche). Protein samples were separated on SDS-polyacrylamide gels. For Western blot, separated proteins were transferred electrophoretically onto nitrocellulose membranes (ISEQ00010, Millipore, Sigma). The membranes were incubated overnight at 4 °C with antibodies against TIMP1 (16644-1-AP) from Proteintech (Rosemont, IL, USA); integrin β1 (sc-59829) and CD63 (sc-5275) from Santa Cruz Biotechnology (Dallas, TX, USA); VE-cadherin (ab33168), pFAK pY397 (ab81298) and total FAK (ab40794) from Abcam (Cambridge, UK); ZO-1 (40−2200), occludin (710192) and claudin-5 (35−2500) from Thermo Fisher Scientific; RhoA (2117) and Na/K ATPase (3010) from Cell Signaling Technology (Danvers, MA, USA). Following anti-mouse or anti-rabbit IgG-HRP (Thermo Fisher Scientific) were used as secondary antibodies for 1 h at room temperature, signals were detected using ImageQuant LAS 4000 (GE Healthcare).

2.11. Cell surface biotinylation assay

HBMECs were biotinylated with 0.5 mg/mL EZ-Link Sulfo−NHS−LC-Biotin (sulfosuccinimidyl-6-[biotin-amido] hexanoate; 21335, Pierce, Carlsbad, CA, USA) in DPBS (137 mmol/L NaCl, 16 mmol/L Na_2HPO_4, 2.7 mmol/L KCl, 1.5 mmol/L KH_2PO_4, 0.5 mmol/L $MgCl_2$, 1 mmol/L $CaCl_2$, pH 7.5) at 4 °C for 30 min, followed by incubating the cells with 100 mmol/L glycine in TBS for an additional 10 min to quench the remaining biotin. Cells were then washed with PBS and lysed in ice-cold lysis buffer (50 mmol/L Tris−HCl pH 7.5, 150 mmol/L NaCl, 1% NP-40) with protease inhibitor mixture at 4 °C for 30 min and centrifuged at $14,000\times g$ for 10 min. Cell extracts were incubated with 20 μL neutravidin beads (29202, Pierce) at 4 °C for 6 h. After incubation, the beads carrying surface proteins were washed with lysis buffer for five times and eluted with 2× loading buffer. The surface proteins were assessed by Western blot analysis.

2.12. Membrane fraction isolation from brain tissue

Mice brain membrane fractions were extracted using a Membrane Protein Extraction Kit (89842, Thermo Fisher) according
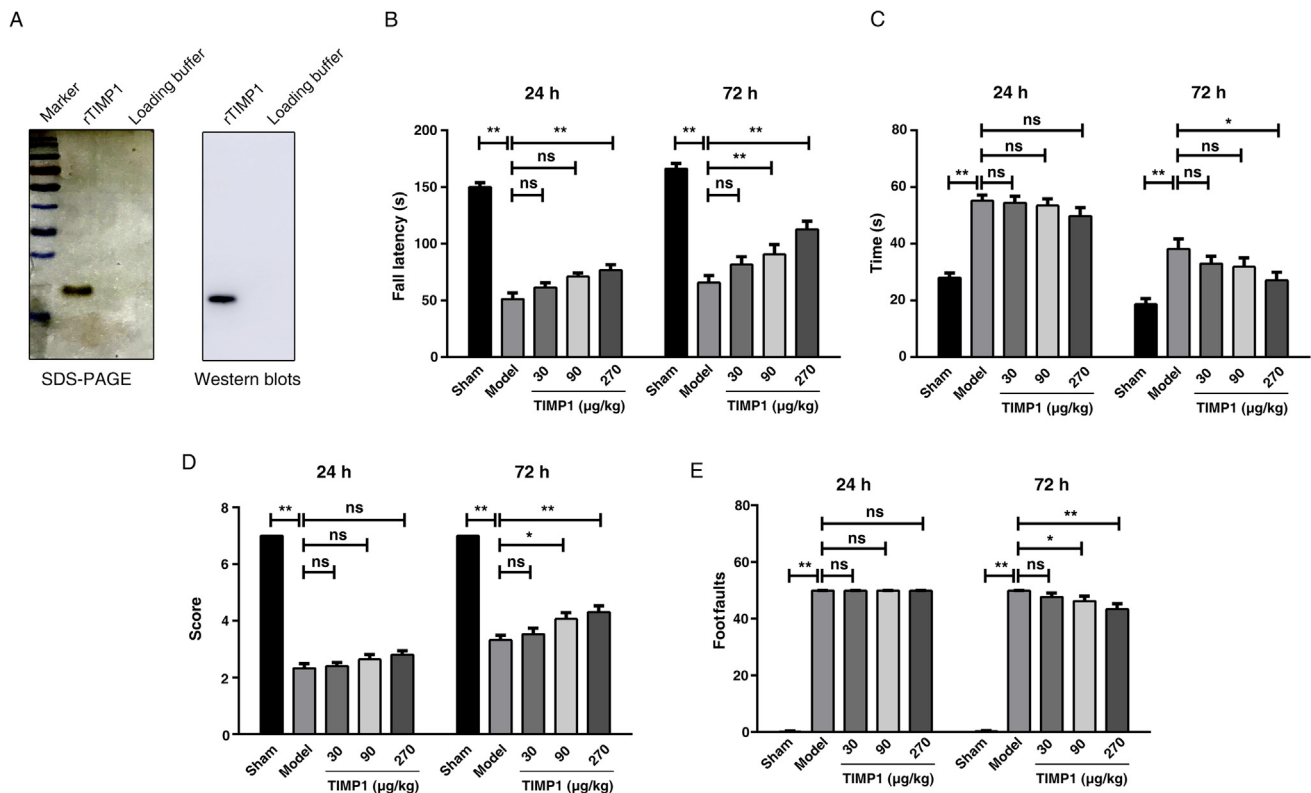
Figure 1 Effects of recombinant TIMP1 (rTIMP1) treatment on neurological outcomes after traumatic brain injury (TBI). (A) Recombinant TIMP1 protein expressed in eukaryotic cells (293T) was analyzed by SDS-PAGE and Western blots analysis. (B)−(E) TBI mice were injected with rTIMP1 (30, 90, and 270 μg/kg) or PBS daily through tail veins. Motor function were assessed at 24 and 72 h post-TBI ($n = 13-15$ per group). (B) Latency to fall from the accelerating Rota-rod. (C) The mean time taken to traverse the beam. (D) Hind limb motor scores in the beam walk test. (E) The number of hind limb foot-faults in the beam walk test. Data are presented as the mean ± SEM (ns, not significant; $^*P < 0.05$; $^{**}P < 0.01$).

to the manufacturer's instructions. Briefly, 40 mg tissue was homogenize in 2 mL permeabilization buffer with protease inhibitor mixture, incubating at 4 °C for 10 min under gentle agitation. The lysates were centrifuged at 16,000× g for 15 min at 4 °C and the pellets were suspended in 1 mL of

solubilization buffer with protease inhibitor mixture. After incubation for 30 min at 4 °C with constant mixing, and then centrifugation at 16,000× g for 15 min, the supernatant containing solubilized membrane was collected for Western blot analysis.
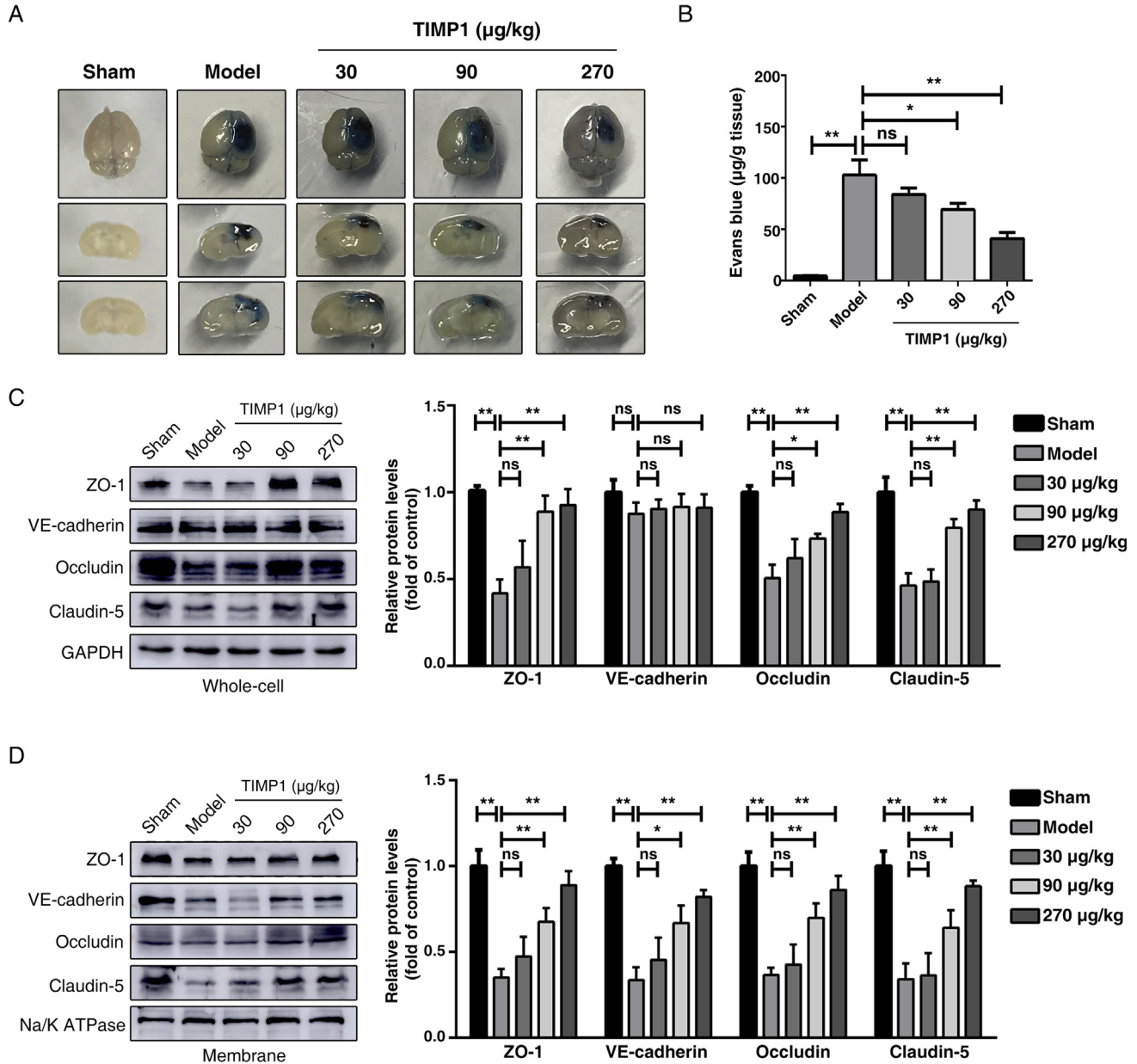

Figure 2 rTIMP1 treatment attenuates blood−brain barrier (BBB) permeability and loss of junctional proteins (JPs) in TBI mice. (A) Representative images of brain tissues and corresponding coronal sections from sham injury group, TBI group treated with vehicle or TBI groups treated with rTIMP1 (30, 90, and 270 μg/kg, i.v.) at 3 days after traumatic brain injury. Blue area indicates extravasation of Evans blue dye. (B) Quantification of the Evans blue dye contents leaking into the ipsilateral cerebral hemisphere tissue of mice from the indicated treatment groups (n = 11−12 per group). (C) Western blot analysis and quantification of ZO-1, VE-cadherin, occludin and claudin-5 in ipsilateral hemispheric brain total lysates from the indicated treatment groups at 72 h post-TBI. GAPDH was used as loading control. n = 5 per group. (D) Western blot analysis and quantification of ZO-1, VE-cadherin, occludin and claudin-5 in ipsilateral hemispheric brain membrane fragments from the indicated treatment groups at 72 h post-TBI. Na/K ATPase was used as loading control. Data are presented as the mean ± SEM, n = 5 per group. (ns, not significant; $^*P < 0.05$; $^{**}P < 0.01$).
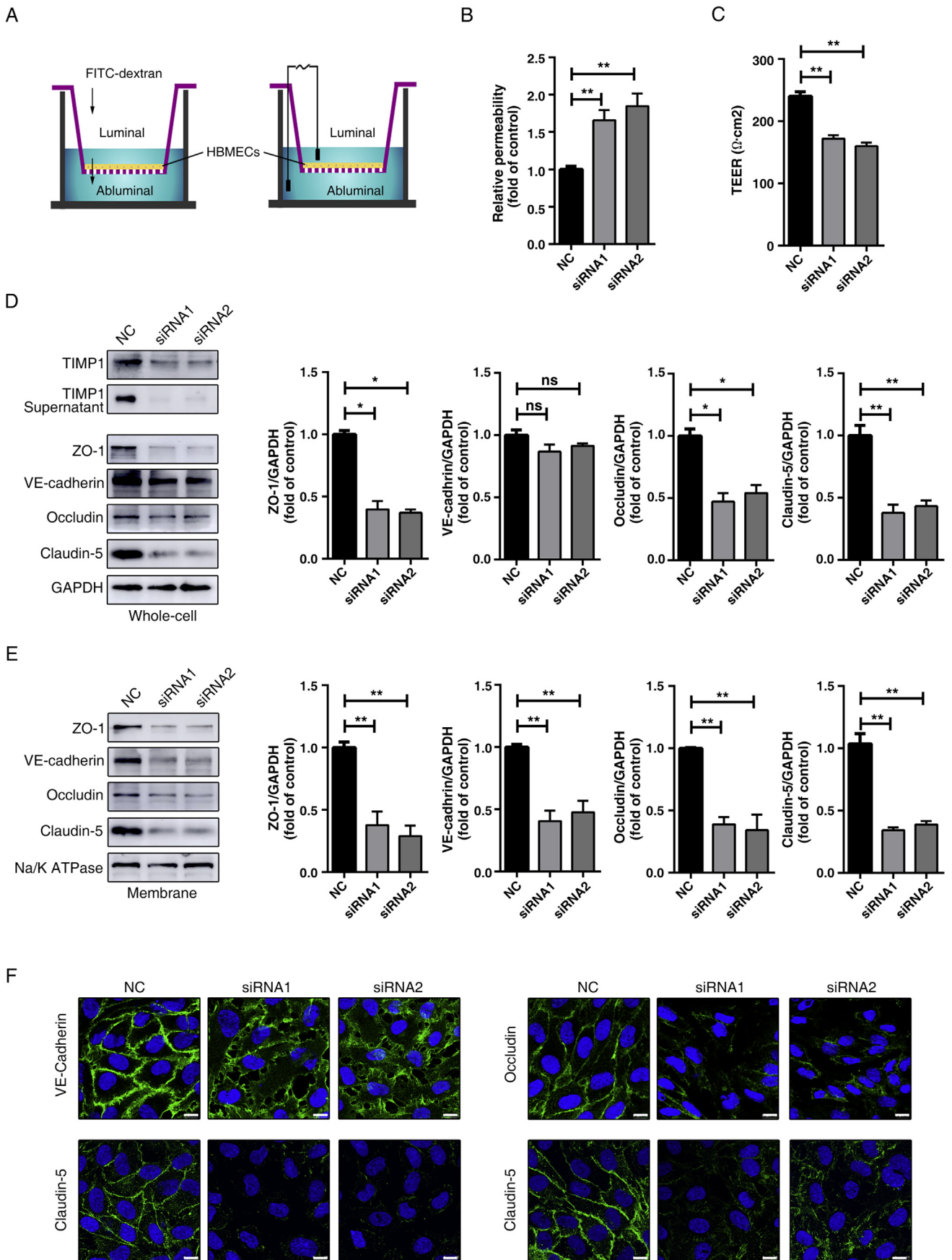
2.13. Immunofluorescence

HBMECs grown on collagen-coated coverslips in 24-well culture plates were washed in PBS and fixed in 4% paraformaldehyde for 15 min at room temperature. Fixed cells were blocked with 5% BSA and permeabilized with 0.1% Triton X-100 for 30 min at room temperature. HBMECs were then immunostained with VE-cadherin (1:200, ab33168, Abcam), claudin-5 (1:100, ab131259, Abcam), ZO-1 (1:50, 40−2200, Thermo Fisher) or occludin (1:100, ab216327, Abcam) diluted in blocking buffer overnight at 4 °C and washed three times with PBS at 5-min intervals. F-actin staining was performed by using Rhodamine-Phalloidin (100 nmol/L, PHDR1, Cytoskeleton, Denver, CO, USA) at room temperature for 1 h. HBMECs were then incubated with Alexa488-anti-rabbit or Alexa488-anti-mouse secondary antibodies (Molecular Probes, Carlsbad, CA, USA) for 1 h followed by counterstaining the nuclear with Hoechst 33342 (1:10000, H1399, Thermo Fisher) for 15 min at room temperature. Images were captured by confocal microscopy using a Leica TCS SP8 (Leica Microsystems, Buffalo Grove, IL, USA).

2.14. Immunoprecipitation

HBMECs were washed with cold PBS and lysed in lysis buffer (50 mmol/L Tris−HCl pH 7.5, 150 mmol/L NaCl, 1% NP-40 and protease inhibitor mixture) on ice for 30 min. After centrifugation at 13,000× g for 20 min at 4 °C, 800 μg cleared extracts were incubated with 3 μg primary antibody or isotype control at 4 °C in a rocker overnight, followed by incubation with protein G-Sepharose 4 Fast Flow beads (17-0618-02, GE Healthcare) for 4 h at 4 °C. Sepharose bound proteins were washed five times with wash buffer (50 mmol/L Tris−HCl pH 7.5, 150 mmol/L NaCl, 0.1% NP-40) and eluted with 2× loading buffer. The immunoprecipitates were assessed by Western blot analysis.

2.15. RhoA activation assay

RhoA activity was measured by using the Rho Activation Assay Biochem Kit (BK036, Cytoskeleton), according to the manufacturer's instructions. Briefly, HBMECs were lysed in cell lysis buffer (50 mmol/L Tris−HCl pH 7.5, 10 mmol/L MgCl₂, 0.5 mol/L NaCl, 2% lgepal) supplemented with protease inhibitor cocktail. Cell lysates were centrifuged, and 25 μg rhotekin-RBD beads were added to 800 μg lysates, followed by incubation at 4 °C in a rocker for 1 h. Beads bound proteins were washed once with wash buffer (25 mmol/L Tris−HCl pH 7.5, 30 mmol/L MgCl₂, 40 mmol/L NaCl) and eluted with 2× loading buffer. The samples were analyzed by Western blotting by using the indicated RhoA antibody.

2.16. Statistical analysis

All data are presented as the mean ± SEM. The differences among three or more groups were determined using one-way ANOVA followed by Bonferroni's multiple comparisons test. Results are presented as mean ± SEM. All analyses were conducted using GraphPad Prism7.00 software (San Diego, CA, USA, RRID: SCR_000306). Differences at $P < 0.05$ were considered statistically significant.

3. Results

3.1. rTIMP1 improves neurobehavioral functions in mice with experimental TBI

To investigate whether TIMP1 exerts protective effects against brain injury, purified rTIMP1 (Fig. 1A) was administered intravenously for 3 consecutive days following TBI. Rotarod test and beam-walking tasks were conducted to evaluate the motor performance. Prior to surgery, there were no differences among the groups for all tests. In rotarod test, TBI induced functional impairment, as indicated by a significant decrease in running time, while rTIMP1 administration (30, 90, and 270 μg/kg) dose-dependently reversed the reduction in time at 24 and 72 h post-TBI (Fig. 1B).

The beam-walking tasks include time to traverse the balance beam, contralateral hindlimb motor scores and the numbers of footfalls. No significant differences were observed among the four TBI groups at 24 h in all tests ($P > 0.05$). Traversing time was generally decreased in all TBI groups because of spontaneous recovery. At 72 h post-TBI, administration of 270 μg/kg rTIMP1 significantly reduced traversing time compared with that of TBI groups (Fig. 1C). Moreover, mice treated with 90 and 270 μg/kg rTIMP1 both increased the hindlimb motor scores (Fig. 1D) and decreased footfalls numbers (Fig. 1E), demonstrating rTIMP1 can rescue the TBI injury-induced motor impairments.

3.2. rTIMP1 treatment attenuates TBI-induced BBB disruption in mice

Previous studies using Timp1⁻/⁻ mice indicated that TIMP1 can regulate vascular permeability[33] and participate in the angiogenic process[18]. We next examined the effect of rTIMP1 on BBB

Figure 3 *TIMP1* knockdown induces trans-endothelial barrier leakage and degradation of endothelial JPs. (A) Illustration of the *in vitro* BBB model to evaluate barrier function. An HBMECs monolayer seeded on top membrane of the cell culture insert followed by measurement of the concentration of 40 kDa FITC-dextran leaking into abluminal to determine the paracellular permeability (left) or the trans-endothelial electrical resistance (TEER) to estimate the TJ integrity (right). (B) HBMECs transfected with control or siRNA against hTIMP1 were subject to transwell permeability assay. Data represent mean ± SEM of six independent experiments (**$P < 0.01$). (C) HBMECs transfected with control or siRNA against hTIMP1 were subject to TEER assay. Data represent mean ± SEM of six independent experiments (**$P < 0.01$). (D) Western blot analysis and quantification of the indicated proteins in total cell lysates of HBMECs treated with siRNA. GAPDH was used as loading control. Data represent mean ± SEM of three independent experiments (ns, not significant; *$P < 0.05$; **$P < 0.01$). (E) Western blot analysis and quantification of the indicated proteins on membrane fragments of HBMECs treated with siRNA. Na/K ATPase was used as loading control. Data represent mean ± SEM of three independent experiments (**$P < 0.01$). (F) The distribution of junctional proteins in HBMECs treated with siRNA were analyzed by immunofluorescence (IF) staining using antibodies against VE-cadherin (green), claudin-5 (green), occludin (green) or claudin-5 (green) and counterstained with Hoechst33342 (blue) for nuclear labelling. Scale bars, 10 μm.

integrity 3 days post-TBI, the time at which BBB is maximally impaired[34]. Evans blue extravasation in the ipsilateral hemisphere was significantly attenuated in rTIMP1-treated animals, compared with that in the vehicle-treated group, as shown visually in Fig. 2A and quantitatively in Fig. 2B.

Because BBB permeability is regulated mainly by the AJs and TJs, we analyzed the total protein homogenates and membrane fractions prepared from tissue surrounding the contusion core, respectively. Western blot analysis revealed that TBI remarkably decreased expression of TJ proteins (ZO-1, occludin, claudin-5) in both whole-cell lysates (Fig. 2C) and plasma membrane fractions (Fig. 2D). Although there was only a slight reduction in the total expression of adherens junction VE-cadherin (Fig. 2C), its amount associated with the membrane fractions was dramatically decreased (Fig. 2D), suggesting that TBI induced VE-cadherin redistribution. However, after rTIMP1 administration (90 and 270 μg/kg), junctional protein levels were significantly increased, compared with those in the vehicle-treated groups (Fig. 2C and D), indicating that rTIMP1 can alleviate TBI-induced loss of TJ proteins.

3.3. TIMP1 knockdown impairs endothelial barrier integrity

To characterize the specific role of TIMP1 in the maintenance of BBB integrity, we applied two different siRNA constructs targeting human TIMP1. Western blot analyses indicated a significant knockdown of *TIMP1* expression in HBMECs. Furthermore, as a secreted protein, TIMP1 levels in the cell culture supernatant were also decreased (Fig. 3D). Trans-endothelial permeability and endothelial tightness were respectively evaluated using FITC-dextran leakage and TEER measurement assays, with an *in vitro* BBB model composed of a monolayer of HBMECs (Fig. 3A). Compared with the control cells, cells with endogenous TIMP1 suppression exhibited subtle paracellular hyperpermeability, with an increase in the luminal to abluminal flux of 40-kDa dextran (Fig. 3B). In addition, *TIMP1* knockdown disrupted BBB tightness, as demonstrated by reduced TEER (Fig. 3C), suggesting that TIMP1 plays an important role in regulating the endothelial barrier.

Since the junctional proteins are essential for maintaining endothelial tightness, we further explored the effects of TIMP1 on the expression and distribution of proteins. Biotin-Avidin system was applied to purify the plasma membrane. Western blot analysis revealed that knockdown of *TIMP1* using two different siRNAs both resulted in decreased levels of TJ proteins, especially in the membrane fractions (Fig. 3D and E). In line with the *in vivo* TBI model results, RNAi-mediated TIMP1 downregulation led to a marked reduction in VE-cadherin levels in the plasma membrane (Fig. 3E), while its expression in whole cell lysates remained unchanged (Fig. 3D).

Consistent with the above Western blot results, immunolabeling analysis further confirmed the effects of TIMP1 on BBB endothelial AJs and TJs. Silencing TIMP1 weakened VE-cadherin expression at extracellular cell−cell contact sites and this expression was increased in the cytosol and, perhaps, in the nuclear compartment as well (Fig. 3F). Regarding TJs (claudin-5, occludin and ZO-1), reduced cytosolic and membrane localization were observed in response to *TIMP1* knockdown (Fig. 3F). Taken together, the data show that TIMP1 is functionally coupled to the expression and subcellular distribution of major junctional elements, thus participating in the maintenance of endothelial barrier integrity under physiological conditions.

3.4. TIMP1 preserves endothelial barrier integrity under hypoxia plus IL-1β insult

In TBI, except for the vascular integrity disruption caused by primary injury, hypoxia[35] and inflammation[36] are two risk factors that contribute to BBB breakdown and secondary injury. We mimicked these *in vivo* scenarios by exposing HBMECs to hypoxic stress plus 20 ng/mL IL-1β for 24 h. Compared to IL-1β stimulation or hypoxia stress alone, Western blot analysis confirmed that their combination is the most suitable *in vitro* model for our studies, since the changes in junctional protein expression and distribution were similar to those in the TBI model (Supporting Information Fig. S1).

Using the *in vitro* model mentioned above, we next applied varying amounts of rTIMP1 to the HBMECs culture and assessed their effects on endothelial barrier regulation under pathological conditions. As shown in Fig. 4A, the paracellular permeability of HBMECs was enhanced significantly after hypoxia plus IL-1β insult, and treatment with rTIMP1 (0.01−3 μg/mL) observably reduced FITC-dextran leakage. Consistent with the dextran extravasation results, the TEER data suggested that hypoxia plus IL-1β decreased endothelial cell resistance, whereas rTIMP1 (0.01−3 μg/mL) administration dose-dependently rescued the low resistance (Fig. 4B). In addition, the expression and distribution of junctional proteins were examined by Western blotting. The results revealed that rTIMP1 at 1 μg/mL could significantly ameliorate these damaging effects by upregulating the total expression of TJs (Fig. 4C), as well as that in the associated membrane fractions (Fig. 4D). Moreover, 1 μg/mL rTIMP1 also increased the amount of VE-cadherin on plasma membrane (Fig. 4D). Similar results were observed in TIMP1 overexpressed endothelial cell (Supporting Information Fig. S2), but not in cells transfected with the mock vector. Collectively, these results not only suggest that TIMP1 can directly regulate BBB integrity, but also indicate that TIMP1 functions as an exogenous molecule at the cell surface after being secreted.

3.5. TIMP1-mediated endothelial barrier integrity is MMP-independent

TIMP1 has a two-domain structure with N- and C-terminal regions. The N-terminal domain harbors MMP-inhibitory sites, while the C-terminal domain plays a significant role in binding to the cell surface. To investigate whether TIMP1 regulates junctional proteins by its metalloproteinase-inhibitory or cytokine-like signaling activities, we performed site-directed mutagenesis to generate a TIMP1 combinatorial mutant with His7Ala and Gln9Ala (Ala-TIMP1), which was shown to disrupt MMP-inhibitory activity but not affect the overall structural integrity or MMP binding[37]. The purified recombinant Ala-TIMP1 (rAla-TIMP1) expressed in eukaryotic cells was identified by SDS-PAGE and Western blotting (Fig. 5A). HBMECs exposed to hypoxia plus IL-1β were treated with rTIMP1 and rAla-TIMP1, respectively, at a concentration of 1 μg/mL. As shown in Fig. 5B, exogenous rTIMP1, with or without MMP-inhibitory activity, ameliorated the FITC-dextran leakage to the same extent. Consistently, rAla-TIMP1 treatment rescued the reduction in TEER as effectively as the wild-type rTIMP1 (Fig. 5C). When junctional protein expression was examined by immunoblot analysis, rAla-TIMP1 abolished the loss of expression in total cell lysates and membrane fractions, as observed in wild-type rTIMP1-
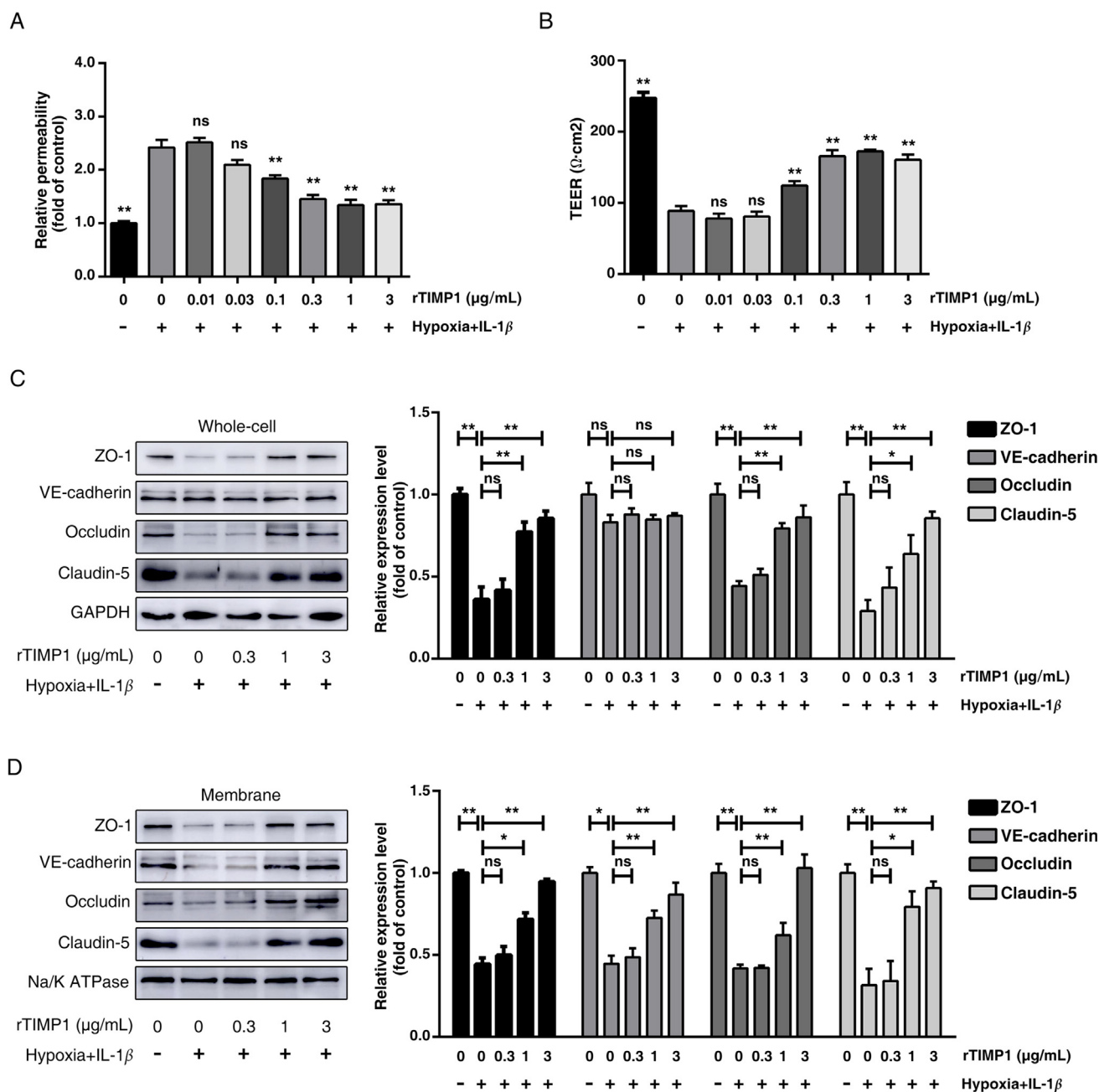
Figure 4 TIMP1 attenuates BBB impairment induced by hypoxia plus IL-1β insult. HBMECs treated with PBS or rTIMP1 at indicated doses were subjected to hypoxia plus 20 ng/mL IL-1β for 24 h. (A) HBMECs from the indicated treatment groups were subject to transwell permeability assay. Data represent mean ± SEM of six independent experiments (ns, not significant; $^{**}P < 0.01$). (B) HBMECs from the indicated treatment groups were subject to TEER assay. Data represent mean ± SEM of six independent experiments (ns, not significant; $^{**}P < 0.01$). (C) Western blot analysis and quantification of ZO-1, occludin, claudin-5 and VE-cadherin protein levels in total cell lysates from the indicated treatment groups. GAPDH was used as loading control. Data represent mean ± SEM of three independent experiments (ns, not significant; $^{*}P < 0.05$; $^{**}P < 0.01$). (D) Western blot analysis and quantification of ZO-1, occludin, claudin-5 and VE-cadherin protein levels on membrane fragments from the indicated treatment groups. Na/K ATPase was used as loading control. Data represent mean ± SEM of three independent experiments (ns, not significant; $^{*}P < 0.05$; $^{**}P < 0.01$).

treated cells (Fig. 5D and E). Immunostaining of cells under hypoxia plus IL-1β insult showed barely detectable VE-cadherin and TJs expression in the cell−cell junctions, compared to that in control cells. However, upon rTIMP1 or rAla-TIMP1 administration, VE-cadherin was redistributed from the cytoplasm to the

cell surface, and TJs expression was increased in both the cytosol and membrane fractions (Fig. 5F). Consequently, TIMP1-mediated BBB regulation appears to be independent of MMP based on the comparable effects between rTIMP1 and rAla-TIMP1 treatment.
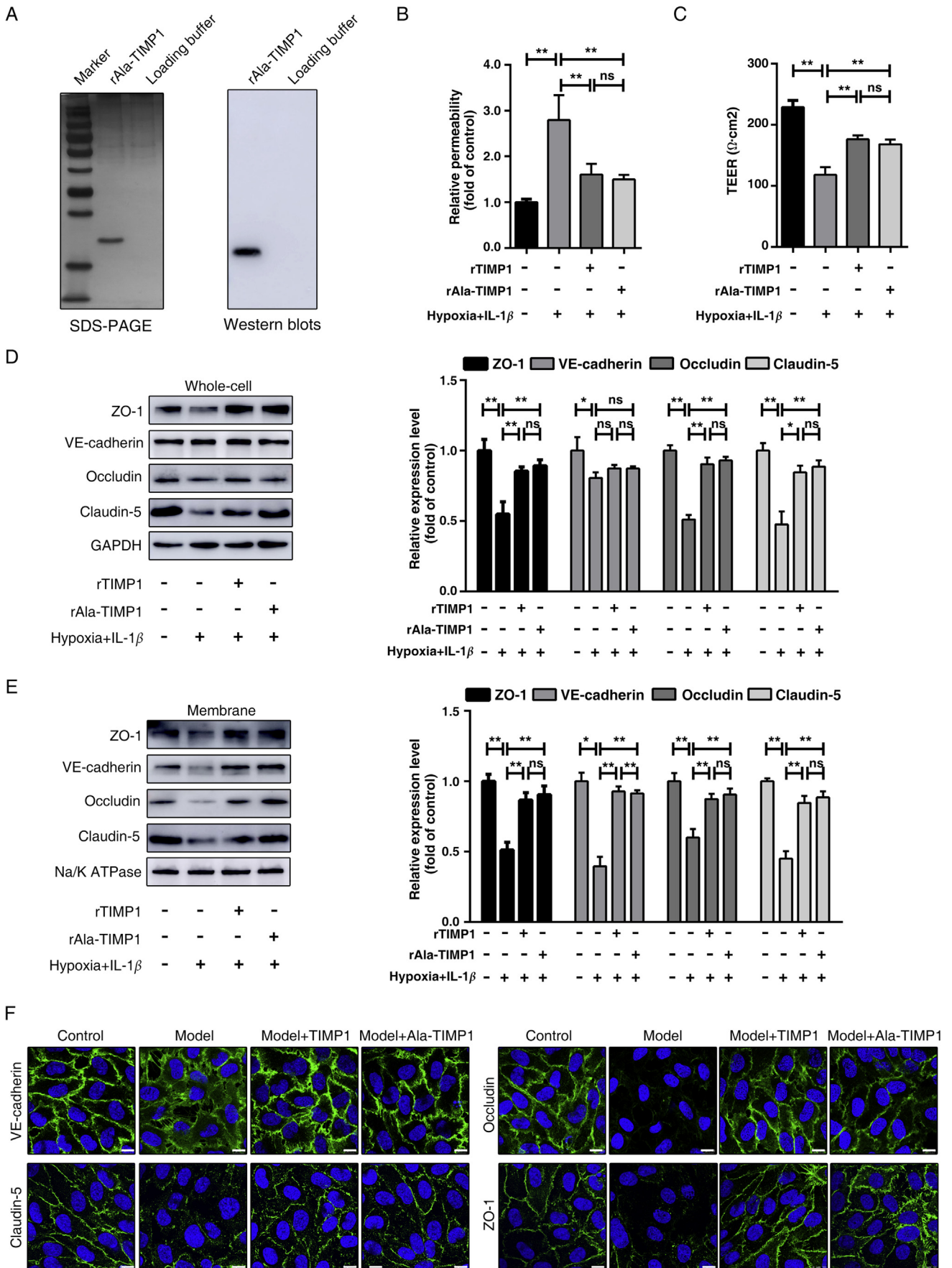
3.6. CD63/integrin β1 complex is essential for TIMP1 regulation of endothelial barrier integrity

Using the TIMP1 mutant, our results revealed that TIMP1 can function as a signaling molecule to regulate endothelial barrier integrity independent of its MMP-inhibitory domain. We next sought to investigate the specific signaling of the "cytokine-like" activity of TIMP1 on endothelial. Previous studies have identified that the C-terminal domain of TIMP1 interacts with the large extracellular loop of CD63, a member of the tetraspanin family, on the cell surface and displays tumor-promoting activities in a CD63-dependent manner[22]. In addition, as the main tetraspanin-interacting integrin, β1 subunit interacts with TIMP1/CD63 complex and plays a critical role in TIMP1-regulated signaling. Therefore, we investigated the potential interaction of TIMP1 and CD63/integrin β1 complex on endothelial cell surface. Anti-TIMP1 antibody-immunoprecipitation (IP) could pull down both CD63 and integrin β1 (Fig. 6A) from HBMECs lysates, meanwhile, CD63 and integrin β1 IP could both pull down TIMP1 (Fig. 6B), suggesting that these proteins form a complex.

Next, we investigated whether CD63/integrin β1 complex is required for TIMP1-mediated BBB integrity. As shown in Fig. 6C, administration of rTIMP1 to cells under hypoxia plus IL-1β rescued the increased diffusion of FITC-dextran across the endothelial barrier. In contrast, downregulated CD63 or integrin β1 expression both abolished the protective effects of TIMP1. Consistently, rTIMP1 failed to prevent TEER reduction in CD63 or integrin β1 knockdown cells (Fig. 6D). These results strongly suggest that CD63/integrin β1 complex is essential for TIMP1-mediated trans-endothelial tightness.

In addition to the *in vitro* BBB model to examine paracellular permeability, we asked whether CD63/integrin β1 complex is required for TIMP1-mediated expression and distribution of junctional proteins. Western blot analysis confirmed significant downregulation of CD63 and integrin β1 expression in HBMECs receiving specific CD63 and integrin β1 siRNA, respectively. Of note, silencing CD63 reduced integrin β1 expression, while the expression level of integrin β1 had little effect on CD63 (Fig. 6E). Both CD63 and integrin β1 knockdown significantly reduced TJs expression in total lysates from rTIMP1 treated cells as determined by Western blotting (Fig. 6E). CD63 or integrin β1 knockdown also abrogated the TIMP1-regulated increase of junctional proteins on cell surface (Fig. 6F). Concordant with Western blot results, immunostaining revealed that rTIMP1 failed to regulate VE-cadherin redistribution and TJs expression when CD63/integrin β1 were downregulated (Fig. 6G), further demonstrating that TIMP1 regulation of endothelial barrier integrity is mediated, at least in part, by its interaction with CD63/integrin β1 complex on cell surface.

3.7. TIMP1 activates Integrin-FAK signaling to modulate F-actin rearrangement

Previous studies revealed that by binding to CD63, TIMP1 may alter CD63 interaction with integrin β1 and in turn influence integrin signaling[21]. Integrins have no intrinsic tyrosine kinase activity and recruit non-receptor tyrosine kinases to activate downstream pathways, including the FAK pathway that restores endothelial barrier function in response to thrombin[38]. Therefore, we analyzed the activation status of FAK in HBMECs exposed to hypoxia plus IL-1β insult after TIMP1 treatment. Evidently, exposure to combined hypoxia plus IL-1β resulted in increased levels of phosphorylated FAK (pFAK) at Tyr397, whereas exogenous addition of rTIMP1 (Fig. 7A) and TIMP1 overexpression (Fig. 7B) both augmented FAK signaling in HBMECs. To investigate whether FAK signaling activation underlies the endothelial barrier regulation of TIMP1, we assessed how Y15, a specific FAK inhibitor, affects HBMECs treated with TIMP1. As the results, Y15 completely abrogated the protective effects of TIMP1 on FITC-dextran leakage (Fig. 7C) and TEER assays (Fig. 7D). In accordance, in our model system, FAK inhibitor significantly reduced TJs expression and reversed redistribution of VE-cadherin in TIMP1-treated cells, as determined by Western blotting (Fig. 7E and F). Importantly, inhibition of FAK significantly reversed the protective effects of exogenous TIMP1 treatment on BBB *in vivo* (Supporting Information Fig. S3). Taken together, these results indicate that TIMP1 activates integrin−FAK signaling to maintain endothelial barrier integrity.

FAK is one of the key proteins that negatively regulate RhoA activation[39], which subsequently induces F-actin stress fiber formation, resulting in contraction-driven endothelial hyperpermeability[40,41]. Next, we used the GST pull-down assay to determine RhoA activity. As shown in Fig. 7G, combined hypoxia plus IL-1β insult clearly increased the amount of active form of RhoA (RhoA-GTP), which was significantly reduced upon rTIMP1 treatment. Similarly, TIMP1 overexpression in HBMECs also alleviated increases in RhoA activity (Fig. 7H), further demonstrating that RhoA is a downstream regulator in the TIMP1-mediated pathway.

RhoA activation triggers robust actin polymerization, followed by the formation of intercellular gaps between endothelial cells and the degradation of junctional proteins[42]. Therefore, we asked whether TIMP1 maintains the endothelial barrier integrity *via* inhibiting RhoA-mediated F-actin rearrangement. Analysis of actin cytoskeleton organization using rhodamine-phalloidin revealed that hypoxia plus IL-1β induced a dramatic increase in F-actin stress fibers across the cells. However, upon TIMP1 stimulation, these fibers dissociated, resulting in the redistribution

Figure 5 TIMP1 protects against BBB injury in an MMP-independent manner. (A) Recombinant rAla-TIMP1 protein expressed in eukaryotic cells (293T) was analyzed by SDS-PAGE and Western blots analysis. (B)−(F) HBMECs treated with 1 μg/mL rTIMP1 or rAla-TIMP1 were subjected to hypoxia plus 20 ng/mL IL-1β for 24 h. (B) HBMECs from the indicated treatment groups were subject to transwell permeability assay. Data represent mean ± SEM of six independent experiments (ns, not significant; $^{**}P < 0.01$). (C) HBMECs from the indicated treatment groups were subject to TEER assay. Data represent mean ± SEM of six independent experiments (ns, not significant; $^{**}P < 0.01$). (D) Western blot analysis and quantification of indicated proteins from total cell lysates (ns, not significant; $^{*}P < 0.05$; $^{**}P < 0.01$). (E) Western blot analysis and quantification of indicated proteins from membrane fragments. Data represent mean ± SEM of three independent experiments (ns, not significant; $^{*}P < 0.05$; $^{**}P < 0.01$). (F) Cells were also subjected to IF staining of VE-cadherin, claudin-5, occludin and ZO-1. Scale bars, 10 μm.
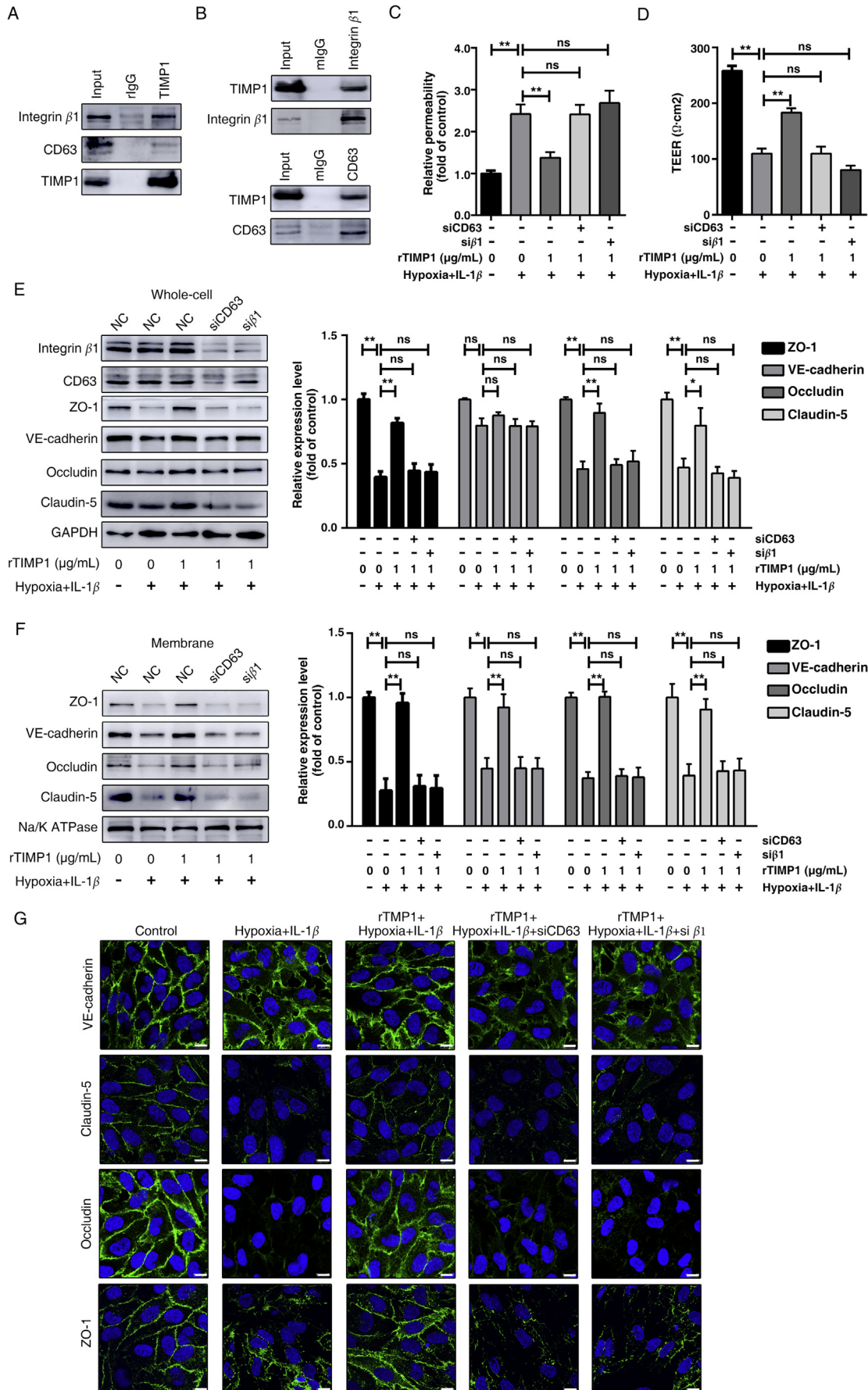
of F-actin to the cell surface, similar to that in the control groups (Fig. 7I and J). Importantly, TIMP1 failed to reverse actin polymerization in CD63-or integrin β1-depleted cells (Supporting Information Fig. S4). Altogether, our results suggest that TIMP1 regulates cytoskeletal reorganization through FAK/RhoA signaling, and CD63/integrin β1 complex is the key mediator.

4. Discussion

In this study, we identified a previously unexplored role of TIMP1 in regulation of endothelial barrier integrity. rTIMP1 exhibits protective effects against BBB breakdown induced by TBI in mice. Silencing TIMP1 in HBMECs induced obvious paracellular permeability and junctional protein deregulation. Using mutagenesis analyses and a cell culture injury model, we determined that TIMP1 maintains BBB integrity through a mechanism independent of its MMP-inhibitory function. Mechanistically, TIMP1 interacts with CD63/integrin β1 complex and activates downstream FAK signaling, leading to the attenuation of RhoA activity, resulting in a decrease in F-actin formation and an increase in cell—cell contact stabilization. Therefore, treatments targeting TIMP1 and the downstream components may pave the way for novel therapies to preserve BBB integrity in CNS diseases, especially in TBI.

The BBB is a unique microvascular structure that plays an important role in maintaining brain homeostasis. BBB breakdown and the associated hyperpermeability are the characteristic features of several CNS diseases[43]. Dysfunction of the BBB induces neurotoxic protein influx from the peripheral blood and immune cell infiltration, which result in a poor neurological prognosis, including cognitive/behavioral disabilities, seizures, coma, and even death. Therefore, treatments that attenuate BBB disruption may be promising therapeutic strategies[44]. It is already known that MMP9 plays a critical role in regulating BBB integrity *via* its proteolytic activities, which are capable of degrading ECM components, promoting neutrophil migration and triggering the inflammatory response[45]. Mice deficient in MMP9 were protected against traumatic[46] and ischemic brain injuries[47]. TIMP1, known as an MMP9 inhibitor, displays an endogenous compensatory response to minimize MMP9 pro-enzyme activity[12]. An imbalance between MMP9 and TIMP1 has been thought to be a key event in the transition from physiological to pathological conditions in various CNS diseases[13−15]. Previous studies have shown that TIMP1 deficiency amplifies vascular permeability in acute lung injury[33] and exacerbates BBB dysfunction in focal cerebral ischemia[16], whereas intracerebroventricular injection of TIMP1 attenuates BBB permeability in acute liver failure[48]. Because BBB

breakdown is an important contributor to TBI pathology and outcomes[49], in the present study, we first evaluated the protective effects of TIMP1 in a mouse model of experimental TBI. The results showed that post-injury TIMP1 treatment improved neurological functions, attenuated Evans blue extravasation, and regulated junctional protein expression and redistribution. To the best of our knowledge, this is the first study demonstrating that rTIMP1 can alleviate BBB breakdown in a TBI model.

Junctional proteins are composed of TJs and AJs that are hallmarks of BBB integrity. Alteration of junctional protein assembly contributes to the loss of BBB integrity. Silencing TIMP1 in HBMECs induced junctional protein dysregulation, leading to an increase in paracellular permeability and a reduction in transendothelial tightness. Consistently, upon hypoxia plus IL-1β insult, exogenous addition and overexpression experiments indicated that TIMP1 is essential for maintaining endothelial barrier integrity in FITC-dextran leakage and TEER assays. These results suggest that TIMP1 can preserve BBB integrity *via* regulating junctional proteins under both physiological and pathological conditions.

TIMP1 was originally characterized as an MMP inhibitor, with a primary role in ECM turnover and remodeling. Previous studies attributed the protective effects of TIMP1 on several *in vivo* models to its MMP-inhibitory activity. However, mounting evidence has revealed that the specific mechanisms of TIMP1 regulation depend on the cell context and the pathological conditions. For example, the anti-apoptotic CD63-mediated function and the anti-proteolytic function of TIMP1 act together in wound healing[28,50], as well in fibrosis progression[19,51]. During EAE, mice overexpressing TIMP1 mitigate the disease course by MMP inhibition in the early stage[25], whereas during chronic EAE, TIMP1 plays an MMP-independent role, potentially by promoting oligodendrocyte differentiation and effective remyelination after injury[26]. Therefore, it is likely that the role of TIMP1 rests on coordinate inhibition of MMP in conjunction with CD63-mediated MMP-independent pathway. TIMP1 is a multifunctional protein with an N-terminal domain for MMP9 inhibition and a C-terminal domain for its interaction with the large extracellular loop of CD63. The sequence between Cys3 and Cys13 within the N-terminal region has shown to be critical for the TIMP1 interaction with MMP9[37]. To maintain the molecular conformation, we introduced His7Ala and Gln9Ala to generate a TIMP1 combinatorial mutant (Ala-TIMP1). TIMP1 and Ala-TIMP1 treatments displayed comparable protective effects on junctional protein regulation and cell permeability, providing evidence that MMP-independent mechanism is involved in the TIMP1-mediated BBB stabilization. However, it is worth noting that this study does not exclude the MMP-inhibitory effect of TIMP1 on BBB regulation.

Figure 6 TIMP1 modulates BBB integrity through CD63 and integrin β1 signaling. (A) Total cell lysates from HBMECs were extracted and subjected to IP assay using TIMP1 antibody. Western blots were performed for integrin β1, CD63 or TIMP1. (B) Total cell lysates from HBMECs were extracted and subjected to integrin β1 or CD63 IP assays. This was followed by Western blot analysis for integrin β1, CD63 or TIMP1. (C)−(H) HBMECs transfected control or siRNA targeting CD63 or integrin β1 were treated with rTIMP1, then the indicated groups were subjected to hypoxia plus 20 ng/mL IL-1β for 24 h. (C) HBMECs from the indicated treatment groups were subject to transwell permeability assay. Data represent mean $\pm$ SEM of six independent experiments (ns, not significant; $^{**}P < 0.01$). (D) HBMECs from the indicated treatment groups were subject to TEER assay. Data represent mean $\pm$ SEM of six independent experiments (ns, not significant; $^{**}P < 0.01$). (E) Western blot analysis and quantification of indicated proteins from total cell lysates (ns, not significant; $^{*}P < 0.05$; $^{**}P < 0.01$). (F) Western blot analysis and quantification of indicated proteins from membrane fragments. Data represent mean $\pm$ SEM of three independent experiments (ns, not significant; $^{*}P < 0.05$; $^{**}P < 0.01$). (G) Cells were also subjected to IF staining of VE-cadherin, claudin-5, occludin and ZO-1. Scale bars, 10 μm.
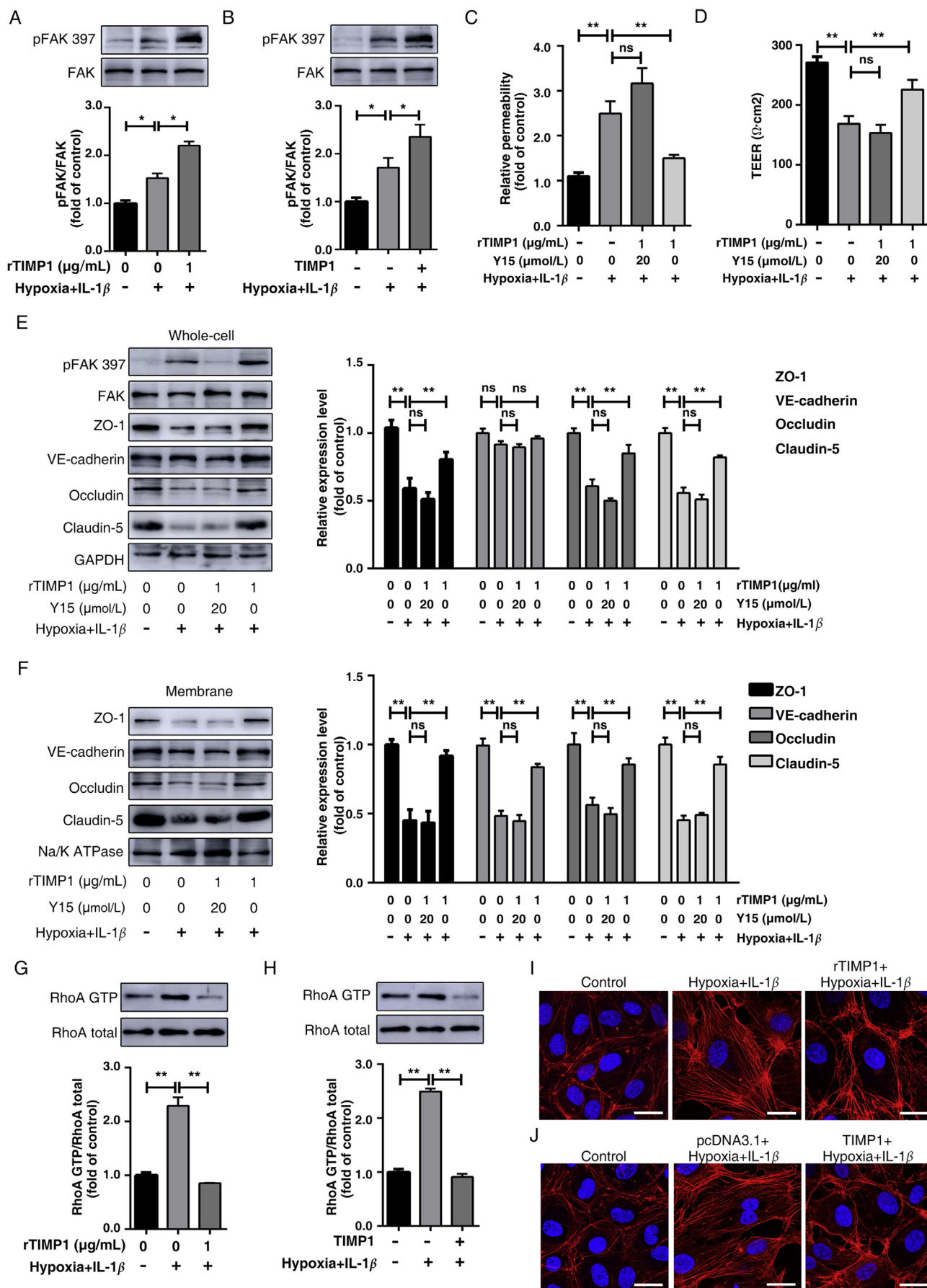
FAK is a cytoplasmic tyrosine kinase that mediates intracellular signaling triggered by integrin complexes[52]. In early studies, due to the activated phosphorylation of FAK in response to the permeability-increasing mediators VEGF[53], thrombin[54] and oxidants[55], FAK was presumed to impair endothelial barrier integrity. However, silencing FAK or expressing FRNK (dominant negative FAK construct) resulted in an augmented and prolonged increase in endothelial permeability, suggesting that FAK activation actually confers a barrier protective property[56]. Consistent with previous reports, a marked increase in FAK phosphorylation was induced by hypoxia plus IL-1β insult in our studies, while TIMP1 treatment further augmented the phosphorylation status *via* activating integrin β1. Holinstat et al.[56] demonstrated that phosphorylated FAK downregulates RhoA-GTP levels *via* p190RhoGAP is a crucial step in endothelial barrier restoration. RhoA activation induced by exposure to specific stressors, such as hypoxia and cytokines, leads to assembly of stress fibers[57,58]. The contraction of stress fibers generates the formation of intercellular gaps between endothelial cells[59], accompanied by the degradation and internalization of junctional proteins[42]. VE-cadherin is an important component of AJs due to its cytoplasmic tail binding to β-catenin to communicate with the cytoskeleton[60,61]. Following exposure to specific stressors, F-actin stress fibers generate centripetal force throughout the cell, which breaks apart the VE-cadherin/β-catenin complex, followed by enhanced nuclear localization of β-catenin, which downregulates claudin-5 transcription[62,63]. Consistent with these findings, there were obvious internalization of VE-cadherin and decreased claudin-5 expression induced by hypoxia plus inflammation insult in our injury model. Moreover, both exogenous addition and overexpression of TIMP1 inhibited RhoA activity and F-actin polymerization, thereby relieving cytoskeletal tension. Of note, the rescue effect of TIMP1 on F-actin stress fiber formation depended on the CD63/integrin β1 complex, further confirming that the MMP-independent mechanism is essential for TIMP1-mediated endothelial barrier integrity.

Nevertheless, we aware that there were some mechanistic caveats may exist. Nowadays, little research on the regulation of ZO-1 and occludin expression by RhoA activity has been carried out. Overexpression of the RhoA-GTP Q63L mutant, a constitutively activated, GTP-bound form of RhoA-GTP, in bEnd.3 cells decreased the expression levels of ZO-1[64]. Moreover, a constitutively active form of RhoA induced the phosphorylation of occludin at Ser490, which is required for occludin ubiquitination and degradation[65,66]. In our studies, the inhibition of RhoA

activity by TIMP1 rescued the decreased expression levels of ZO-1 and occludin. Further studies were warranted to elucidate the specific mechanisms underlying the regulation of ZO-1 and occludin expression by TIMP1. In addition, only *in vitro* experiments were applied to reveal that TIMP1 preserves BBB integrity *via* interacting with CD63/integrin β1 complex. It is necessary to perform TBI model on mice with conditional knockout for CD63 or integrin β1 in endothelial cells to further confirm the regulatory mechanism of TIMP1 on BBB. Finally, although *in vivo* TBI experiments using FAK inhibitor significantly reversed the protective effects of exogenous TIMP1 treatment on BBB *in vivo*, suggesting that FAK/RhoA signaling plays an important role in TIMP1-mediated BBB protection, a better strategy would likely be use of mice conditional knockout for FAK to avoid the nonspecific inhibition or incomplete inhibition of the inhibitor, and mice with *Mmp9* knockout will better confirm that TIMP1 maintains BBB function *via* MMP-independent pathway.

BBB breakdown is the hallmark of TBI and several other neurological disorders, and a better understanding and control of the mechanisms involved in BBB disruption hold promise for improving patient care. As junctional proteins govern much of the BBB function, focus on these proteins as therapeutic targets may be beneficial. Although early studies have found that MMP9 expression was upregulated when the BBB was damaged and the use of MMP9 antibodies could alleviate the BBB leakage. However, MMP9 inhibitors, particularly those with hydroxamate bases, have not been widely used in clinical practice due to their low specificity and poor solubility. Moreover, it has been reported that MMP9 participated in the injury process early after onset while contributed to recovery during later stages[67]. Therefore, the treatment window for MMP9 inhibitors is another obstacle in clinical applications. In our studies, we uncovered that besides MMP-dependent pathway, TIMP1 also regulated BBB integrity *via* an MMP-independent pathway. The new finding will provide more strategies for CNS diseases with BBB disruption.

5. Conclusions

Taken together, our studies uncovered that TIMP1 regulates endothelial barrier integrity through its interaction with CD63/integrin β1 complex on the cell surface and integrin signaling activation. The subsequent inhibition of RhoA activity stabilizes

Figure 7 TIMP1 activates Integrin-FAK signaling to modulate F-actin rearrangement. (A) HBMECs treated with PBS or rTIMP1 at 1 µg/mL were subjected to hypoxia plus 20 ng/mL IL-1β for 24 h. Western blot analysis and quantification of phosphorylated FAK levels in cell lysates. Data represent mean $\pm$ SEM of three independent experiments ($^*P < 0.05$). (B) HBMECs transfected with pcDNA3.1 or TIMP1 were subjected to hypoxia plus 20 ng/mL IL-1β for 24 h. Western blot analysis and quantification of phosphorylated FAK levels in cell lysates. Data represent mean $\pm$ SEM of three independent experiments ($^*P < 0.05$). (C)−(F) HBMECs treated with PBS, 20 µmol/L Y15 and 1 µg/mL TIMP1, or 1 µg/mL TIMP1 alone were subjected to hypoxia plus 20 ng/mL IL-1β for 24 h. Transwell permeability (C) and TEER (D) assays were performed. Data represent mean $\pm$ SEM of six independent experiments (ns, not significant; $^*P < 0.05$; $^{**}P < 0.01$). Western blot analysis and quantification of indicated proteins from total cell lysates (E) and membrane fragments (F). Data represent mean $\pm$ SEM of five independent experiments (ns, not significant; $^*P < 0.05$; $^{**}P < 0.01$). (G) HBMECs treated with PBS or rTIMP1 at 1 µg/mL were subjected to hypoxia plus 20 ng/mL IL-1β for 24 h. Western blot analysis and quantification of RhoA-GTP levels in cell lysates. Data represent mean $\pm$ SEM of three independent experiments ($^*P < 0.05$). (H) HBMECs transfected with pcDNA3.1 or TIMP1 were subjected to hypoxia plus 20 ng/mL IL-1β for 24 h. Western blot analysis and quantification of RhoA-GTP levels in cell lysates. Data represent mean $\pm$ SEM of three independent experiments ($^*P < 0.05$). (I) HBMECs treated with PBS or rTIMP1 at 1 µg/mL were subjected to hypoxia plus 20 ng/mL IL-1β for 24 h, and were subjected to IF staining of F-actin. Scale bars, 25 µm. (J) HBMECs transfected with pcDNA3.1 or TIMP1 were subjected to hypoxia plus 20 ng/mL IL-1β for 24 h, and were subjected to IF staining of F-actin. Scale bars, 25 µm.

cytoskeleton, providing protection against endothelial barrier disruption, which is induced by permeability-increasing mediators. The present study identifies TIMP1 as an extracellular signal inducer that exhibits cytokine-like activities in maintaining BBB function and integrity. This novel MMP-independent mechanism of TIMP1 in endothelial provides insight into BBB disruption under pathological conditions. Moreover, the protective effects of rTIMP1 in an *in vivo* TBI model imply that targeting TIMP1 and its downstream signaling may provide novel therapeutic strategies for CNS diseases with BBB sealing deficiency.

Acknowledgments

Author contributions

Jingshu Tang and Ying Peng designed the experiments. Jingshu Tang and Longjian Huang conducted the majority of biological experiments. Jingshu Tang and Yuying Kang conducted the *in vivo* experiments. Yuying Kang and Lei Wu analyzed the data. Jingshu Tang drafted the manuscript. Ying Peng conceived and supervised the project. Jingshu Tang and Ying Peng participated in data analysis and wrote and finalized the manuscript writing.

Conflicts of interest

All authors declare that there is no conflict of interest in this study.

Appendix A.   Supporting information

Supporting data to this article can be found online at https://doi.org/10.1016/j.apsb.2020.02.015.

References

1. Alluri H, Wiggins-Dohlvik K, Davis ML, Huang JH, Tharakan B. Blood−brain barrier dysfunction following traumatic brain injury. *Metab Brain Dis* 2015;**30**:1093−104.
2. Cheng C, Yu Z, Zhao S, Liao Z, Xing C, Jiang Y, et al. Thrombospondin-1 gene deficiency worsens the neurological outcomes of traumatic brain injury in mice. *Int J Med Sci* 2017;**14**:927−36.
3. Neuwelt EA, Bauer B, Fahlke C, Fricker G, Iadecola C, Janigro D, et al. Engaging neuroscience to advance translational research in brain barrier biology. *Nat Rev Neurosci* 2011;**12**:169−82.
4. Korczyn AD. Vascular parkinsonism—characteristics, pathogenesis and treatment. *Nat Rev Neurol* 2015;**11**:319−26.
5. Drouin-Ouellet J, Sawiak SJ, Cisbani G, Lagace M, Kuan WL, Saint-Pierre M, et al. Cerebrovascular and blood−brain barrier impairments in Huntington's disease: potential implications for its pathophysiology. *Ann Neurol* 2015;**78**:160−77.
6. Zenaro E, Piacentino G, Constantin G. The blood−brain barrier in Alzheimer's disease. *Neurobiol Dis* 2017;**107**:41−56.
7. Ortiz GG, Pacheco-Moises FP, Macias-Islas MA, Flores-Alvarado LJ, Mireles-Ramirez MA, Gonzalez-Renovato ED, et al. Role of the blood−brain barrier in multiple sclerosis. *Arch Med Res* 2014;**45**:687−97.
8. Dietrich W, Erbguth F. Increased intracranial pressure and brain edema. *Med Klin Intensivmed Notfallmed* 2013;**108**:157−69.
9. Thal SC, Neuhaus W. The blood−brain barrier as a target in traumatic brain injury treatment. *Arch Med Res* 2014;**45**:698−710.
10. Obermeier B, Verma A, Ransohoff RM. The blood−brain barrier. *Handb Clin Neurol* 2016;**133**:39−59.
11. Woessner Jr JF. Matrix metalloproteinases and their inhibitors in connective tissue remodeling. *FASEB J* 1991;**5**:2145−54.
12. Ries C. Cytokine functions of TIMP-1. *Cell Mol Life Sci* 2014;**71**:659−72.
13. Ichiyama T, Siba P, Suarkia D, Takasu T, Miki K, Kira R, et al. Serum levels of matrix metalloproteinase-9 and tissue inhibitors of metalloproteinases 1 in subacute sclerosing panencephalitis. *J Neurol Sci* 2007;**252**:45−8.
14. Palus M, Zampachova E, Elsterova J, Ruzek D. Serum matrix metalloproteinase-9 and tissue inhibitor of metalloproteinase-1 levels in patients with tick-borne encephalitis. *J Infect* 2014;**68**:165−9.
15. Li DD, Song JN, Huang H, Guo XY, An JY, Zhang M, et al. The roles of MMP-9/TIMP-1 in cerebral edema following experimental acute cerebral infarction in rats. *Neurosci Lett* 2013;**550**:168−72.
16. Fujimoto M, Takagi Y, Aoki T, Hayase M, Marumo T, Gomi M, et al. Tissue inhibitor of metalloproteinases protect blood−brain barrier disruption in focal cerebral ischemia. *J Cerebr Blood Flow Metabol* 2008;**28**:1674−85.
17. Magnoni S, Baker A, Thomson S, Jordan G, George SJ, McColl BW, et al. Neuroprotective effect of adenoviral-mediated gene transfer of TIMP-1 and -2 in ischemic brain injury. *Gene Ther* 2007;**14**:621−5.
18. Mandel ER, Uchida C, Nwadozi E, Makki A, Haas TL. Tissue inhibitor of metalloproteinase 1 influences vascular adaptations to chronic alterations in blood flow. *J Cell Physiol* 2017;**232**:831−41.
19. Takawale A, Zhang P, Patel VB, Wang X, Oudit G, Kassiri Z. Tissue inhibitor of matrix metalloproteinase-1 promotes myocardial fibrosis by mediating CD63-integrin beta1 interaction. *Hypertension* 2017;**69**:1092−103.
20. Gomis-Ruth FX, Maskos K, Betz M, Bergner A, Huber R, Suzuki K, et al. Mechanism of inhibition of the human matrix metalloproteinase stromelysin-1 by TIMP-1. *Nature* 1997;**389**:77−81.
21. Jung KK, Liu XW, Chirco R, Fridman R, Kim HR. Identification of CD63 as a tissue inhibitor of metalloproteinase-1 interacting cell surface protein. *EMBO J* 2006;**25**:3934−42.
22. Cui H, Seubert B, Stahl E, Dietz H, Reuning U, Moreno-Leon L, et al. Tissue inhibitor of metalloproteinases-1 induces a pro-tumourigenic increase of miR-210 in lung adenocarcinoma cells and their exosomes. *Oncogene* 2015;**34**:3640−50.
23. Forte D, Salvestrini V, Corradi G, Rossi L, Catani L, Lemoli RM, et al. The tissue inhibitor of metalloproteinases-1 (TIMP-1) promotes survival and migration of acute myeloid leukemia cells through CD63/PI3K/Akt/p21 signaling. *Oncotarget* 2017;**8**:2261−74.
24. Lee SY, Kim JM, Cho SY, Kim HS, Shin HS, Jeon JY, et al. TIMP-1 modulates chemotaxis of human neural stem cells through CD63 and integrin signalling. *Biochem J* 2014;**459**:565−76.
25. Althoff GE, Wolfer DP, Timmesfeld N, Kanzler B, Schrewe H, Pagenstecher A. Long-term expression of tissue-inhibitor of matrix metalloproteinase-1 in the murine central nervous system does not alter the morphological and behavioral phenotype but alleviates the course of experimental allergic encephalomyelitis. *Am J Pathol* 2010;**177**:840−53.
26. Crocker SJ, Whitmire JK, Frausto RF, Chertboonmuang P, Soloway PD, Whitton JL, et al. Persistent macrophage/microglial activation and myelin disruption after experimental autoimmune encephalomyelitis in tissue inhibitor of metalloproteinase-1-deficient mice. *Am J Pathol* 2006;**169**:2104−16.
27. Stilley JA, Sharpe-Timms KL. TIMP1 contributes to ovarian anomalies in both an MMP-dependent and -independent manner in a rat model. *Biol Reprod* 2012;**86**:1−10.
28. Caley MP, Martins VL, O'Toole EA. Metalloproteinases and wound healing. *Adv Wound Care (New Rochelle)* 2015;**4**:225−34.
29. Chen SF, Hsu CW, Huang WH, Wang JY. Post-injury baicalein improves histological and functional outcomes and reduces inflammatory

cytokines after experimental traumatic brain injury. *Br J Pharmacol* 2008;**155**:1279−96.

30. Shaw KE, Bondi CO, Light SH, Massimino LA, McAloon RL, Monaco CM, et al. Donepezil is ineffective in promoting motor and cognitive benefits after controlled cortical impact injury in male rats. *J Neurotrauma* 2013;**30**:557−64.

31. Fox GB, Fan L, Levasseur RA, Faden AI. Sustained sensory/motor and cognitive deficits with neuronal apoptosis following controlled cortical impact brain injury in the mouse. *J Neurotrauma* 1998;**15**:599−614.

32. Zhou X, Wu Y, Ye L, Wang Y, Zhang K, Wang L, et al. Aspirin alleviates endothelial gap junction dysfunction through inhibition of NLRP3 inflammasome activation in LPS-induced vascular injury. *Acta Pharm Sin B* 2019;**9**:711−23.

33. Kim KH, Burkhart K, Chen P, Frevert CW, Randolph-Habecker J, Hackman RC, et al. Tissue inhibitor of metalloproteinase-1 deficiency amplifies acute lung injury in bleomycin-exposed mice. *Am J Respir Cell Mol Biol* 2005;**33**:271−9.

34. Yang Y, Rosenberg GA. Blood−brain barrier breakdown in acute and chronic cerebrovascular disease. *Stroke* 2011;**42**:3323−8.

35. Yan EB, Satgunaseelan L, Paul E, Bye N, Nguyen P, Agyapomaa D, et al. Post-traumatic hypoxia is associated with prolonged cerebral cytokine production, higher serum biomarker levels, and poor outcome in patients with severe traumatic brain injury. *J Neurotrauma* 2014;**31**:618−29.

36. Murray KN, Parry-Jones AR, Allan SM. Interleukin-1 and acute brain injury. *Front Cell Neurosci* 2015;**9**:1−17.

37. O'Shea M, Willenbrock F, Williamson RA, Cockett MI, Freedman RB, Reynolds JJ, et al. Site-directed mutations that alter the inhibitory activity of the tissue inhibitor of metalloproteinases-1: importance of the N-terminal region between cysteine 3 and cysteine 13. *Biochemistry* 1992;**31**:10146−52.

38. Mehta D, Tiruppathi C, Sandoval R, Minshall RD, Holinstat M, Malik AB. Modulatory role of focal adhesion kinase in regulating human pulmonary arterial endothelial barrier function. *J Physiol* 2002;**539**:779−89.

39. Schmidt TT, Tauseef M, Yue L, Bonini MG, Gothert J, Shen TL, et al. Conditional deletion of FAK in mice endothelium disrupts lung vascular barrier function due to destabilization of RhoA and Rac1 activities. *Am J Physiol Lung Cell Mol Physiol* 2013;**305**:L291−300.

40. Kim JG, Islam R, Cho JY, Jeong H, Cap KC, Park Y, et al. Regulation of RhoA GTPase and various transcription factors in the RhoA pathway. *J Cell Physiol* 2018;**233**:6381−92.

41. Burridge K, Wittchen ES. The tension mounts: stress fibers as force-generating mechanotransducers. *J Cell Biol* 2013;**200**:9−19.

42. Shi Y, Zhang L, Pu H, Mao L, Hu X, Jiang X, et al. Rapid endothelial cytoskeletal reorganization enables early blood−brain barrier disruption and long-term ischaemic reperfusion brain injury. *Nat Commun* 2016;**7**:10523.

43. Zhao Z, Nelson AR, Betsholtz C, Zlokovic BV. Establishment and dysfunction of the blood−brain barrier. *Cell* 2015;**163**:1064−78.

44. Obermeier B, Daneman R, Ransohoff RM. Development, maintenance and disruption of the blood−brain barrier. *Nat Med* 2013;**19**:1584−96.

45. Pla-Navarro I, Bevan D, Hajihosseini MK, Lee M, Gavrilovic J. Interplay between metalloproteinases and cell signalling in blood brain barrier integrity. *Histol Histopathol* 2018;**33**:1253−70.

46. Wang X, Jung J, Asahi M, Chwang W, Russo L, Moskowitz MA, et al. Effects of matrix metalloproteinase-9 gene knock-out on morphological and motor outcomes after traumatic brain injury. *J Neurosci* 2000;**20**:7037−42.

47. Asahi M, Wang X, Mori T, Sumii T, Jung JC, Moskowitz MA, et al. Effects of matrix metalloproteinase-9 gene knock-out on the proteolysis of blood−brain barrier and white matter components after cerebral ischemia. *J Neurosci* 2001;**21**:7724−32.

48. Chen F, Radisky ES, Das P, Batra J, Hata T, Hori T, et al. TIMP-1 attenuates blood−brain barrier permeability in mice with acute liver failure. *J Cerebr Blood Flow Metabol* 2013;**33**:1041−9.

49. Chodobski A, Zink BJ, Szmydynger-Chodobska J. Blood−brain barrier pathophysiology in traumatic brain injury. *Transl Stroke Res* 2011;**2**:492−516.

50. Boulday G, Fitau J, Coupel S, Soulillou JP, Charreau B. Exogenous tissue inhibitor of metalloproteinase-1 promotes endothelial cell survival through activation of the phosphatidylinositol 3-kinase/Akt pathway. *Ann N Y Acad Sci* 2004;**1030**:28−36.

51. Murphy FR, Issa R, Zhou X, Ratnarajah S, Nagase H, Arthur MJ, et al. Inhibition of apoptosis of activated hepatic stellate cells by tissue inhibitor of metalloproteinase-1 is mediated *via* effects on matrix metalloproteinase inhibition: implications for reversibility of liver fibrosis. *J Biol Chem* 2002;**277**:11069−76.

52. Schlaepfer DD, Mitra SK. Multiple connections link FAK to cell motility and invasion. *Curr Opin Genet Dev* 2004;**14**:92−101.

53. Abedi H, Zachary I. Vascular endothelial growth factor stimulates tyrosine phosphorylation and recruitment to new focal adhesions of focal adhesion kinase and paxillin in endothelial cells. *J Biol Chem* 1997;**272**:15442−51.

54. Carbajal JM, Gratrix ML, Yu CH, Schaeffer Jr RC. ROCK mediates thrombin's endothelial barrier dysfunction. *Am J Physiol Cell Physiol* 2000;**279**:C195−204.

55. Vepa S, Scribner WM, Parinandi NL, English D, Garcia JG, Natarajan V. Hydrogen peroxide stimulates tyrosine phosphorylation of focal adhesion kinase in vascular endothelial cells. *Am J Physiol* 1999;**277**:L150−8.

56. Holinstat M, Knezevic N, Broman M, Samarel AM, Malik AB, Mehta D. Suppression of RhoA activity by focal adhesion kinase-induced activation of p190RhoGAP: role in regulation of endothelial permeability. *J Biol Chem* 2006;**281**:2296−305.

57. Zieseniss A. Hypoxia and the modulation of the actin cytoskeleton—emerging interrelations. *Hypoxia (Auckl)* 2014;**2**:11−21.

58. Schnoor M, Garcia Ponce A, Vadillo E, Pelayo R, Rossaint J, Zarbock A. Actin dynamics in the regulation of endothelial barrier functions and neutrophil recruitment during endotoxemia and sepsis. *Cell Mol Life Sci* 2017;**74**:1985−97.

59. Komarova Y, Malik AB. Regulation of endothelial permeability *via* paracellular and transcellular transport pathways. *Annu Rev Physiol* 2010;**72**:463−93.

60. Giannotta M, Trani M, Dejana E. VE-cadherin and endothelial adherens junctions: active guardians of vascular integrity. *Dev Cell* 2013;**26**:441−54.

61. Abu Taha A, Schnittler HJ. Dynamics between actin and the VE-cadherin/catenin complex: novel aspects of the ARP2/3 complex in regulation of endothelial junctions. *Cell Adhes Migrat* 2014;**8**:125−35.

62. Taddei A, Giampietro C, Conti A, Orsenigo F, Breviario F, Pirazzoli V, et al. Endothelial adherens junctions control tight junctions by VE-cadherin-mediated upregulation of claudin-5. *Nat Cell Biol* 2008;**10**:923−34.

63. Meister S, Storck SE, Hameister E, Behl C, Weggen S, Clement AM, et al. Expression of the ALS-causing variant hSOD1(G93A) leads to an impaired integrity and altered regulation of claudin-5 expression in an *in vitro* blood−spinal cord barrier model. *J Cerebr Blood Flow Metabol* 2015;**35**:1112−21.

64. Park JC, Baik SH, Han SH, Cho HJ, Choi H, Kim HJ, et al. Annexin A1 restores Abeta$_{1-42}$-induced blood−brain barrier disruption through the inhibition of RhoA−ROCK signaling pathway. *Aging Cell* 2017;**16**:149−61.

65. Gopalakrishnan S, Raman N, Atkinson SJ, Marrs JA. Rho GTPase signaling regulates tight junction assembly and protects tight junctions during ATP depletion. *Am J Physiol* 1998;**275**:C798−809.

66. Murakami T, Felinski EA, Antonetti DA. Occludin phosphorylation and ubiquitination regulate tight junction trafficking and vascular endothelial growth factor-induced permeability. *J Biol Chem* 2009;**284**:21036−46.

67. Yang Y, Rosenberg GA. Matrix metalloproteinases as therapeutic targets for stroke. *Brain Res* 2015;**1623**:30−8.